THE JOURNAL OF BIOLOGICAL CHEMISTRY VOL. 283, NO. 17, pp. 11625–11632, April 25, 2008

Amino Acid Residues That Confer High Selectivity of the α6 Nicotinic Acetylcholine Receptor Subunit to α-Conotoxin MII[S4A,E11A,L15A]*

Received for publication, December 18, 2007, and in revised form, February 15, 2008 Published, JBC Papers in Press, February 25, 2008, DOI 10.1074/jbc.M710288200

Layla Azam[‡1], **Doju Yoshikami**[‡], **and J. Michael McIntosh**[‡§]

From the Departments of [‡]*Biology and* [§]*Psychiatry, University of Utah, Salt Lake City, Utah 84112*

Nicotinic acetylcholine receptors (nAChRs) containing α3 and β2 subunits are found in autonomic ganglia and mediate ganglionic transmission. The closely related α6 nAChR subtype is found in the central nervous system where changes in its level of expression are observed in Parkinson's disease. To obtain a ligand that discriminates between these two receptors, we designed and synthesized a novel analog of α-conotoxin MII, MII[S4A,E11A,L15A], and tested it on nAChRs expressed in *Xenopus* oocytes. The peptide blocked chimeric α6/α3β2β3 nAChRs with an IC_{50} of 1.2 nM; in contrast, its IC_{50} on the closely related α3β2 as well as non-α6 nAChRs was three orders of magnitude higher. We identified the residues in the receptors that are responsible for their differential sensitivity to the peptide. We constructed chimeras with increasingly longer fragments of the N-terminal ligand binding domain of the α3 subunit inserted into the homologous positions of the α6 subunit, and these were used to determine that the region downstream of the first 140 amino acids was involved. Further mutagenesis of this region revealed that the α6 subunit residues Glu-152, Asp-184, and Thr-195 were critical, and replacement of these three residues with their homologs from the α3 subunit increased the IC_{50} of the peptide by >1000-fold. Conversely, when these key residues in α3 were replaced with those from α6, the IC_{50} decreased by almost 150-fold. Similar effects were seen with other α6-selective conotoxins, suggesting the general importance of these α6 residues in conferring selective binding.

Nicotinic acetylcholine receptors (nAChRs)[2] are members of the large family of Cys-loop ligand-gated ion channels (1). They are pentameric proteins composed of α subunits alone (homopentamers) or α in combination with β subunits (heteropentamers). In the case of the heteromeric receptors, different combinations of α and β subunits yield receptors with different pharmacological and electrophysiological properties (2). To date, nine α and three β subunits have been discovered and cloned from mammalian nervous tissue. Of these, α2 through α6 can form receptors in combination with β2 through β4, leading to a large assortment of different receptor subtypes.

The α6 subunit has a limited distribution within the brain, largely being expressed by catecholaminergic neurons (3, 4) at presynaptic endings where its activity modulates release of dopamine (5, 6) and norepinephrine (7). Chronic exposure to nicotine has been shown to selectively affect the expression and function of nAChRs on striatal dopaminergic terminals containing this subunit (8–10). Furthermore, α6 nAChRs appear to play a role in the pathophysiology of Parkinson's disease, a disease involving the loss of dopaminergic neurons. In animal models of Parkinson's disease, 1-methyl 4-phenyl 1,2,3,6-tetrahydropyridine-induced injury of dopaminergic neurons is associated with a selective loss of α6*[3] nAChRs in both rodents and monkeys (10–12). In addition, there is selective loss of α6 nAChRs in human Parkinson's disease. Thus, ligands that selectively target α6β2* nAChRs potentially represent a novel class of therapeutic agents (13).

However, it is difficult to pharmacologically distinguish α3β2 from α6β2* nAChRs due to the close structural similarities of the α subunits. α3β2* nAChRs are found on peripheral autonomic ganglia where they modulate cardiac and enteric functions (14, 15). Therapeutic agents targeting CNS α6β2* nAChRs would need to be devoid of activity on α3β2 nAChRs to avoid cardiovascular and intestinal side effects. α-Conotoxin (CTX) MII, a 16-amino acid peptide, is the signature ligand for α6β2* nAChRs; however, α-CTX MII also blocks α3β2 nAChRs with high affinity (16). This is not surprising, given the overall high sequence homology between α6 and α3 subunits and the conservation of residues responsible for interaction with α-CTX MII (17). In this study, we created a novel ligand, based on α-CTX MII, that discriminates between α6/α3β2β3 and α3β2 nAChRs by a factor of 1000 (α6/α3 is a chimera that contains the N-terminal binding region of the α6 subunit and the remaining fragment of the α3 subunit, see "Experimental Procedures"). We constructed receptor chimeras and mutants and determined the non-homologous residues near the ligand binding sites of α6 and α3 that are responsible for this selectivity. The results of the present study provide insight into the nAChR-ligand interaction and may aid in development of α6* nAChR-selective therapeutics.

EXPERIMENTAL PROCEDURES

Materials—Acetylcholine chloride, atropine, and bovine serum albumin were obtained from Sigma. α-CTXs were syn-

* This work was supported by Kirschstein-National Research Service Award Postdoctoral Fellowship DA 016835 (to L. A.) and by National Institutes of Health Grant MH53631 (to J. M. M.) and Grant GM48677 (to D. Y.). The costs of publication of this article were defrayed in part by the payment of page charges. This article must therefore be hereby marked "*advertisement*" in accordance with 18 U.S.C. Section 1734 solely to indicate this fact.

[1] To whom correspondence should be addressed: Dept. of Biology, University of Utah, 257 South 1400 East, Salt Lake City, UT 84112. Tel.: 801-581-5907; Fax: 801-585-5010; E-mail: layla_azam@yahoo.com.

[2] The abbreviations used are: nAChR, nicotinic acetylcholine receptor; AChBP, acetylcholine-binding protein; CTX, conotoxin; NTR, N-terminal binding region; CI, confidence interval.

[3] Asterisk indicates presence of additional subunits.

TABLE 1

Sequences of primers used to construct chimeras and point mutants

For the chimeras, the numbering reflects the length of the α3 N-terminal fragment substituted into the corresponding region of the α6 subunit. For the point mutants, the first amino acid designates the wild-type residue at the numbered location that is replaced with the second amino acid, which is found at the location in the opposite subunit (α3 in case of α6/α3 and α6/α3 in case of α3).

Chimera/mutant	Primer
$\alpha3_{1-140}\alpha6/\alpha3$	5′-TTCCCATTCGACTACCAAAACTGCACCCTGAAATTTGGGTCCTGGACTTACGAC-3′
$\alpha3_{1-160}\alpha6/\alpha3$	5′-AAGATCGACCTGGTCCTCATCGGCTCCAAAGTGGACATGAACGACTTTTGGGAA-3′
$\alpha3_{1-170}\alpha6/\alpha3$	5′-ATGAACCTCAAGGACTACTGGGAGAGTAGTGAGTGGGAAATTGTCGATGCCTCT-3′
$\alpha3_{1-180}\alpha6/\alpha3$	5′-AAACATGAAATCAAGTACAACTGCTGTGAAGAGATTTACACAGATATCACCTAC-3′
α6E152K/α3	5′-GGACTTACGACAAGGCTAAGATCGACCTTCTCATC-3′
α6D184E/α3	5′-TCTGGCTACAAGCATGAAATCAAGTACAACTGC-3′
α6T195Q/α3	5′-TGTGAAGAGATTTACCAAGATATCACCTACTCC-3′
α3K152E	5′-CGACAAGGCAGAAATCGACCTGGTCCTCATCGGCTC-3′
α3E184D	5′-GGCTACAAACATGACATCAAGTACAAC-3′
α3Q195T	5′-TGTGAGGAGATCTACACAGACATCACGTACTCG-3′

thesized as described previously (16, 18, 19). Clones of α2–α7 and β2–β4 cDNAs were kindly provided by S. Heinemann (Salk Institute, San Diego, CA). Clones of β2 and β3 subunits in the high expressing pGEMHE vector were kindly provided by Chuck Luetje (University of Miami, Miami, FL). cDNA clones encoding rat α9 and α10 were provided by Belen Elgoyhen (Universidad de Buenos Aires, Argentina).

Construction of Chimeras—Chimeras were made by PCR using the primer sequences shown in Table 1. Because the α6 subunit does not form functional receptors, we used a functional surrogate formed by splicing the N-terminal extracellular ligand-binding region of the α6 subunit with the remaining fragment of the α3 subunit as previously described (19). Hence, all chimeras of α6 used in this study had portions of the N-terminal ligand-binding region of the α6 subunit replaced with the corresponding region of the α3 subunit. The notation for these chimeras is the length of the α3 sequence at the N-terminal portion, followed by the remaining α6/α3 sequence, which makes up the C-terminal portion. Primers were designed to amplify each length of the extracellular region of the α3 subunit plus a 25-bp 3′-overhang homologous to the remaining extracellular region of the α6 subunit. Similarly, each α6/α3 subunit fragment was amplified that contained a 25-bp 5′-overhang homologous to the α3 subunit. Amplifications of the α3 and α6/α3 fragments were carried out by using *Taq* DNA polymerase (Promega, Madison, WI). Each corresponding α3 and α6/α3 PCR fragment (containing the overhangs) was first hybridized and subsequently extended by PCR, using primers specific for a 5′-segment of the α3 sequence (containing an *NotI* site: 5′-AAGGAAAAAAGCGGCCGCGACATGGGT-GTTGTGCTGCTC-3′) and a 3′-segment of the α6/α3 sequence (containing an *XbaI* site: 5′-GTCCATCTAGACACAGGT-GAGCCTCGATG-3′), using *PfuTurbo* DNA polymerase (Stratagene, La Jolla, CA). The amplified $\alpha3_{1-x}\alpha6/\alpha3$ PCR products were cloned into pT7TS plasmid (a modified pGEM4Z plasmid containing a 5′ and a 3′ *Xenopus* globin untranslated region), using the *NotI* and *SpeI* sites. The ligated products were transformed into either DH10B or HB101 competent cells and grown overnight, and the cDNA was isolated using a miniprep kit (Qiagen, Valencia, CA) and subsequently sequenced.

Construction of Point Mutations—Point mutants were made by PCR using primers shown in Table 1. Primers containing the desired point mutation flanked by 15 bases on either side were synthesized. Using the non-strand displacing action of *PfuTurbo* DNA polymerase, the mutagenic primers were extended and incorporated by PCR. The methylated, non-mutated parental cDNA was digested with *DpnI*. The mutated DNA was transformed into DH10B or DH5α competent cells and isolated using the Qiagen miniprep kit and sequenced to ascertain the incorporation of the desired mutation.

cRNA Preparation and Injection—Capped cRNA for the various subunits were made using the mMessage mMachine *in vitro* transcription kit (Ambion, Austin, TX) following linearization of the plasmid. The chimeras/point mutants made from the original α6/α3 chimera were linearized with *SalI*, and point mutants originally made from the α3 subunit were linearized with *EcoRI*, and transcribed with T7 and SP6, respectively. The cRNA was purified using an RNeasy kit (Qiagen). The concentration of cRNA was determined by absorbance at 260 nm. cRNA of each chimera and point mutant were combined with cRNA of high expressing β2 and β3 subunits (in the pGEMHE vector) to give 167–500 ng/μl of each subunit cRNA. 100 nl of this mixture was injected into each *Xenopus* oocyte with a Drummond microdispenser (Drummond Scientific, Broomall, PA), as described previously (16), and incubated at 17 °C. Oocytes were injected within 1 day of harvesting, and recordings were made 2–4 days post-injection.

Voltage Clamp Recording—Oocytes were voltage-clamped and exposed to ACh and peptide as described previously (16). Briefly, the oocyte chamber consisting of a cylindrical well (~30 μl in volume) was gravity-perfused at a rate of ~2 ml/min with ND-96 buffer (96.0 mM NaCl, 2.0 mM KCl, 1.8 mM $CaCl_2$, 1.0 mM $MgCl_2$, 5 mM HEPES, pH 7.1–7.5) containing 1 μM atropine and 0.1 mg/ml bovine serum albumin. In the case of the α9α10 subtype, the ND96 contained no Mg^{2+} and no atropine, and the oocytes were incubated in 1,2-bis(2-aminophenoxy)ethane-*N*,*N*,*N*′,*N*′-tetraacetic acid tetrakis (acetoxymethyl ester) for 3–4 h prior to recording. The oocyte was subjected once a minute to a 1-s pulse of 100 μM ACh. For screening of receptor chimeras and mutants, for toxin concentrations of 1 μM and lower, once a stable baseline was achieved, either ND-96 alone or ND-96 containing varying concentrations of the α-conotoxins was perfusion-applied, during which 1-s pulses of 100 μM ACh were applied every minute until a constant level of block was achieved. For toxin concentrations of 10 μM and higher, the buffer flow was stopped and the toxin was bath-applied and allowed to incubate with the oocyte for 5 min, after which the ACh pulse was resumed.

ACh Dose Response—To acquire ACh dose-response data, the conventional oocyte chamber was replaced by a chamber

constructed from a disposable 200-μl polypropylene pipette tip with a length of 50 mm and an internal diameter of 0.5 mm at the upstream or intake end and 5 mm at the downstream or exhaust end. The chamber was mounted horizontally with its intake end connected to the perfusion supply, while its exhaust end had a vertical meniscus whose location was dictated by the tip of a sipper made from a 27-gauge hypodermic needle connected to a vacuum line. The chamber had two apertures in its dorsal wall: 1) a 1.5-mm circular hole centered 13 mm downstream from the intake, and 2) a 2.5 × 5 mm (longitudinal) oval centered 14 mm downstream from the hole (*i.e.* a total of 27 mm from the intake end). The oocyte was introduced into the chamber through the oval aperture and secured against the chamber floor by the two voltage clamp glass microelectrodes that impaled the oocyte. The chamber was perfused at a rate of ~2 ml/min. To introduce ACh into the chamber, the perfusion was halted and 20 μl of ACh was manually applied to the chamber via the small circular hole upstream from the oocyte. This volume was too small for ACh to reach the oocyte unless the perfusion was resumed. Upon resumption of perfusion (which was started immediately following the introduction of ACh into the chamber), the bolus of ACh rapidly engulfed the oocyte and washed past it in a matter of seconds, as judged by the time course of ACh response. This process was repeated with different concentrations of ACh with a time interval between applications long enough to avoid desensitization.

Data Analysis—For the baseline response, at least three ACh responses were averaged. To determine the percent block induced by toxin, two to three ACh responses, obtained after a steady-state block had been achieved, were averaged, and the value was divided by the pre-toxin baseline value to yield a % response. The dose-response data were fit to the equation, $Y = 100/(1 + 10\text{^}((\log EC_{50} - \log[\text{Toxin}]) \times n_H))$, where n_H is the Hill coefficient, by non-linear regression analysis using GraphPad Prism (GraphPad Software, San Diego, CA). Each data point is mean ± S.E.M. from at least three oocytes. For ACh dose-response curves, the response to a given ACh concentration was normalized to the response to 100 μM ACh, which served as an internal control.

RESULTS

α-CTX MII[S4A,E11A,L15A] Is a Selective Antagonist of α6 nAChRs*—α-CTX MII is a two-disulfide bridge peptide with the sequence, GCCSNPVCHLEHSNLC-amide. It has high, but similar, potency in blocking both α6β2- and α3β2-containing nAChRs (IC_{50} values of 0.39 and 2.2 nM, respectively (19)). Structure-function studies of α-conotoxin MII indicate that several of the non-Cys residues are less important for activity against α6 *versus* α3 nAChRs (19). We replaced three of these residues, Ser-4, Glu-11, and Leu-15, with Ala and tested them against heterologously expressed α3β2 and α6/α3β2β3 nAChRs. Because the α6 subunit does not form functional receptors, we used a functional surrogate formed by splicing the N-terminal extracellular ligand-binding region of the α6 subunit with the remaining fragment of the α3 subunit. The pharmacology of this chimera has previously been shown to match that of native α6β2* nAChRs for α-CTX MII binding (19). The combined Ala substitutions resulted in a peptide with >600-fold lower activity against α3β2 nAChRs but only 3-fold lower activity against α6/α3β2β3 nAChRs compared with native α-CTX MII (Table 2). Thus, the resulting analog has >1000-fold preference for α6/α3β2β3 over α3β2 nAChRs (Table 2). The rate of recovery from block was slower for α6/α3β2β3 than for α3β2 nAChRs (Fig. 1). A 1-min wash was sufficient for recovery of α3β2 nAChRs, whereas full recovery of α6/α3β2β3 nAChRs required a 5-min wash. Table 2 also shows the effect of α-CTX MII[S4A,E11A,L15A] on other subtypes of rat nAChRs.

Amino Acids Downstream of the First 140 Residues of the N-terminal Region of the α6 Subunit Confer the High Preference of α-CTX MII[S4A,E11A,L15A] for α6/α3β2β3 versus α3β2

TABLE 2

IC_{50} values for block of various rat nAChR subtypes by α-CTX MII[S4A,E11A,L15A]

CI, confidence interval; n_H, Hill coefficient.

nAChR	IC_{50}	95% CI	n_H
	nM		
α6/α3β2β3	1.2	1.1–1.4	1.1 ± 0.06
α3β2	100	1,100–1,900	0.8 ± 0.07
α3β4	380	300–490	1.1 ± 0.09
α4β2	>10,000		
α2β2	>10,000		
α4β4	>10,000		
α2β4	>10,000		
α7	~10,000		
α9α10	>10,000		

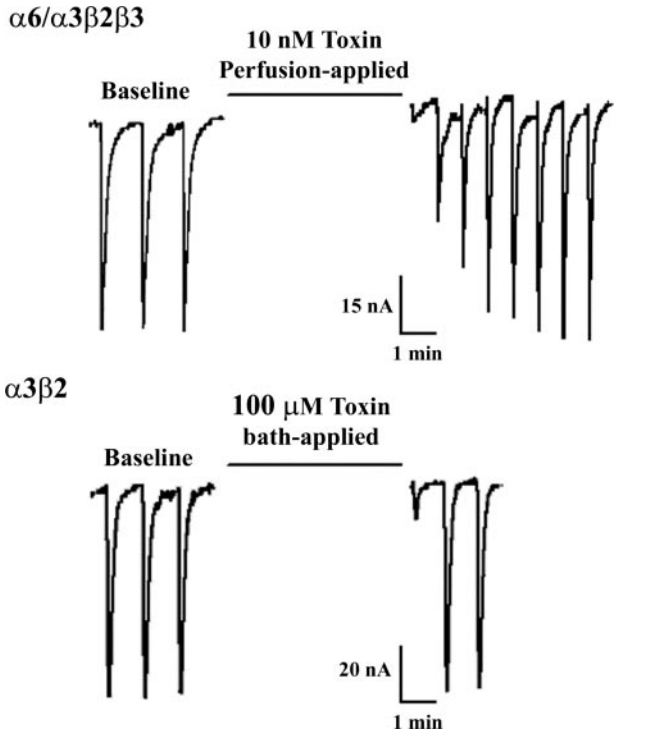

FIGURE 1. **α-CTX MII[S4A,E11A,L15A] differentially blocks α6/α3β2β3 and α3β2 nAChRs.** Oocytes expressing α6/α3β2β3 nAChRs (*top series*) and α3β2 nAChRs (*bottom series*) were voltage clamped at −70 mV and subjected to a 1-s pulse of 100 μM ACh every minute as described under "Experimental Procedures". In each series, the first three responses are controls, following which the oocyte was exposed to the toxin as indicated. The perfusion and ACh pulses were then resumed to monitor the recovery from block during washout of toxin. The toxin was more potent in blocking α6/α3β2β3 than α3β2 nAChRs (note 10^4-fold difference in toxin concentration) (see also Fig. 3). Likewise, the block of α6/α3β2β3 nAChRs was more slowly reversible than that of α3β2 nAChRs.

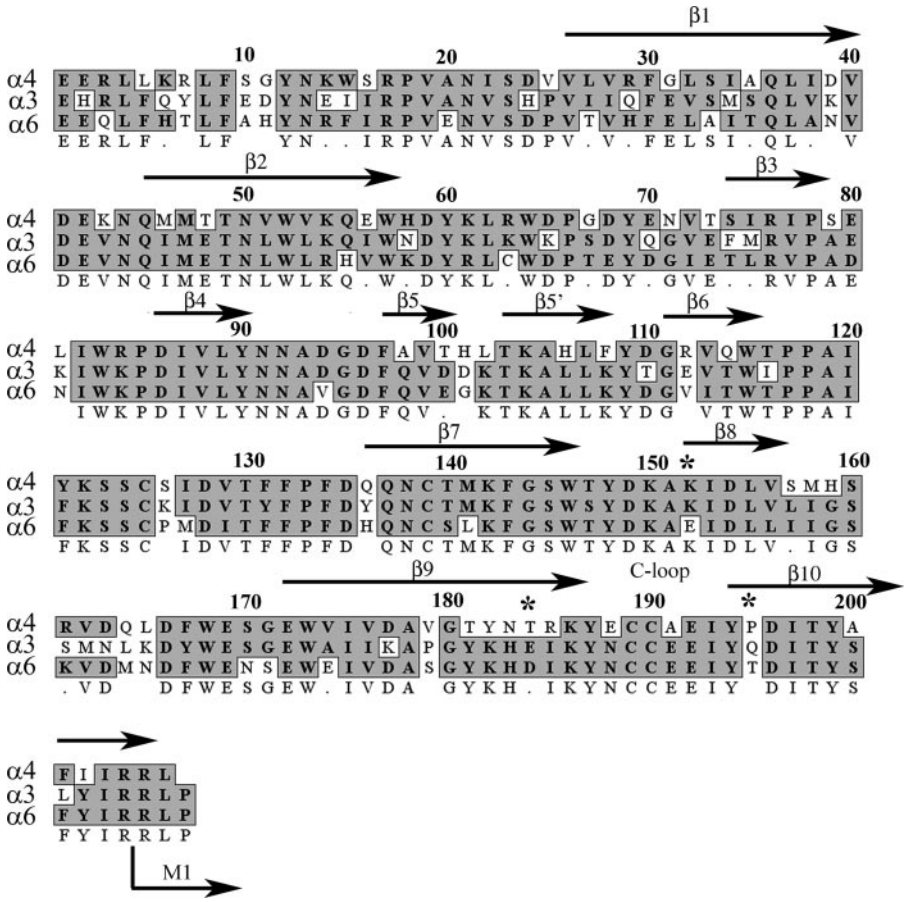

FIGURE 2. **Alignment of N-terminal binding regions of α3, α4, and α6 nAChR subunits.** The conserved residues are outlined in *gray*. The β-sheets (from Refs. 22 and 27) are indicated by *arrows*. Note the substantial homology. The making of the mutant subunits was guided by noting the homologous residues between α3 and α4 subunits that differ from the α6 subunit. The residues that confer high selectivity of α-CTX MII[S4A,E11A,L15A] for the α6 subunit are indicated by an *asterisk*. The start of the first transmembrane domain is indicated by "*M1*."

TABLE 3

IC_{50} values for α-CTX MII[S4A,E11A,L15A] on different chimeras

CI, confidence interval; n_H, Hill coefficient.

Chimera	IC_{50}	95% CI	n_H
	nM		
α6/α3β2β3	1.2	1.1–1.4	1.1 ± 0.06
α3β2	1400	1100–1880	0.8 ± 0.07
$\alpha3_{1-140}\alpha6/\alpha3b2b3$	1.5	1.2–1.9	0.75 ± 0.05
$\alpha3_{1-160}\alpha6/\alpha3b2b3$	58	50–67	0.91 ± 0.05
$\alpha3_{1-170}\alpha6/\alpha3b2b3$	67	61–74	0.93 ± 0.03
$\alpha3_{1-180}\alpha6/\alpha3b2b3$	300	200–460	0.57 ± 0.06

nAChR—The N-terminal binding region (NTR) of α6 and α3 nAChR subunits displays ~80% homology (Fig. 2). To determine the residues responsible for the differential interaction with the peptide, a series of chimeras were constructed, each with a progressively longer fragment of the NTR of the α6 subunit replaced by the corresponding region of the α3 subunit. Replacing the first 140 amino acids of the α6 subunit with the α3 subunit ($\alpha3_{1-140}\alpha6/\alpha3$) did not affect the IC_{50} (Table 3). However, replacing the first 160 residues ($\alpha3_{1-160}\alpha6/\alpha3$) decreased the potency of the toxin by ~50-fold (Table 3), suggesting interaction of the toxin with amino acids located between residues 140 and 160 of the α6 NTR. Replacing an additional 10 amino acids of the α6 subunit with the α3 subunit ($\alpha3_{1-170}\alpha6/\alpha3$) changed the susceptibility to the peptide only slightly. However, exchanging the first 180 amino acids ($\alpha3_{1-180}\alpha6/\alpha3$; 24 amino acids shy of the entire NTR) further shifted the IC_{50} of the toxin toward that of the WT α3β2 nAChR (Table 3). These results suggest that amino acids downstream of the first 140 residues of the α6 subunit confer the high selectivity of α-CTX MII[S4A,E11A,L15A] for α6/α3β2β3 nAChRs.

Glu-152, Asp-184, and Thr-195 of α6 Subunit Interact with α-CTX MII [S4A,E11A,L15A]—Spanning the region between residues 140 and 160 of the NTR are 5 amino acids that differ between the α6 and the α3 subunits (Fig. 2). To determine which residues of the α3 subunit should be substituted into the α6 subunit, the NTR of both α3 and α6 subunits were aligned with that of the α4 subunit, which does not show affinity for the α-CTX MII analog (Fig. 2). Of the five residues that differ between the α6 and α3 subunits in the first 140–160 amino acids, three are shared by both α3 and α4 subunits (Met-141, Lys-152, and Val-156) and one is different in all three (Leu-157 in α3, which is a Ser in α4 and an Ile in α6). When each of these α3 residues was systematically substituted for the corresponding residue in α6, the α6Glu-152 substitution with Lys created the most substantial rightward shift in the dose-response curve, decreasing the potency of the α-CTX MII[S4A,E11A,L15A] for the α6/α3β2β3 mutant receptor by 8-fold relative to that of the WT receptor (Table 4).

The next stretch of amino acids that affected potency of α-CTX MII[S4A,E11A,L15A] was located in the region downstream of the first 170 amino acids (Table 3). Once again, residues that differed between the α6 and the α3 subunits, but were common to the α3 and the α4 subunits, were exchanged. There are 8 amino acids that differ between the α6 and α3 subunits in the region between residues 170 and 204 (Fig. 2). Although α6Val-176 (Ile in α3), α6Asp-177 (Lys in α3) and α6Phe-201 (Leu in α3) differ in the two subunits, they are shared by the α6 and α4 subunits and therefore were not examined. Of the eight different residues, only one is shared by α3 and α4 subunits (Gly-171). However, substituting this residue for Ser found in the α6 NTR did not markedly affect the susceptibility of the receptor to toxin. As for the remaining residues, only substitutions of α6Asp-184 to Glu and α6Thr-195 to Gln decreased the receptor's susceptibility to α-CTX MII[S4A,E11A,L15A], by 8-fold and 9-fold, respectively (Table 4). When the three resi-

TABLE 4

IC_{50} values for α-CTX MII[S4A,E11A,L15A] on mutant nAChRs

CI, confidence interval; n_H, Hill coefficient. The three residue changes that have the largest effect on the IC_{50}, and were subsequently changed simultaneously, are shown in bold.

Mutant nAChR	IC_{50}	95% CI	n_H
	nM		
α6/α3β2β3	1.2	1.1–1.4	1.1 ± 0.06
α3β2	1400	1100–1900	0.8 ± 0.07
α6L141M/α3β2β3	2.8	1.9–4.1	0.86 ± 0.12
α6E152K/α3β2β3	**9.9**	**6.7–15**	**0.83 ± 0.13**
α6L155V/α3β2β3	2.0	1.8–2.1	1.1 ± 0.04
α6I156L/α3β2β3	3.1	2.9–3.4	1.1 ± 0.03
α6S171G/α3β2β3	2.3	2.0–2.7	1.3 ± 0.09
α6E174A/α3β2β3	1.7	1.4–2.1	0.98 ± 0.09
α6S179P/α3β2β3	2.4	2.2–2.6	1.1 ± 0.04
α6D184E/α3β2β3	**10**	**8.8–11**	**1.1 ± 0.07**
α6T195Q/α3β2β3	**11**	**9.0–14**	**1.0 ± 0.1**
α6E152KD184ET195Q/α3β2β3	2100	1200–3600	0.53 ± 0.09
α3K152EE184DQ195Tβ2	9.7	7.6–13	0.96 ± 0.08

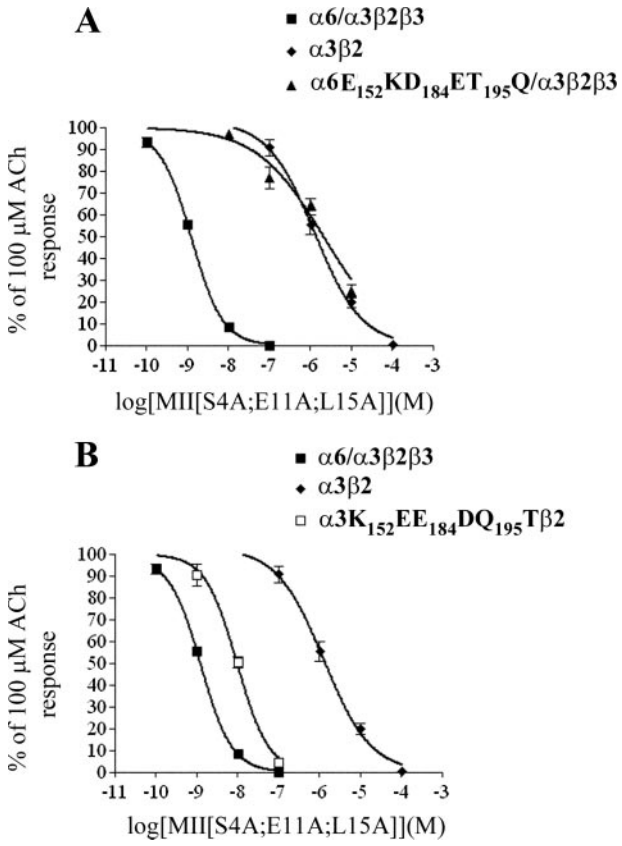

FIGURE 3. **Differential susceptibility of α6/α3β2β3 *versus* α3β2 nAChRs to α-CTX MII[S4A,E11A,L15A] is due largely to three residues.** Oocytes expressing one of four different nAChRs were voltage clamped and subjected to ACh pulses as described in Fig. 1 and "Experimental Procedures." *A*, combined mutations of the three identified residues in the extracellular binding region of the α6 subunit decreased sensitivity to α-CTX MII[S4A,E11A,L15A] by >1000-fold. *B*, substitution of the three α3 residues with the homologous α6 residues yielded a receptor that was 150-fold more sensitive to the α-CTX MII analog compared with WT α3β2 nAChR. Values are mean ± S.E.M. from three to five separate oocytes.

dues that markedly affected the potency of the α-CTX MII analog were simultaneously changed (α6E152KD184ET195Q/α3), the IC_{50} of α-CTX MII[S4A,E11A,L15A] for the triple receptor mutant was approximately equal to the IC_{50} obtained for the WT α3β2 receptor (Table 4 and Fig. 3*A*).

To ascertain whether the decreased toxin susceptibility of the α6E152KD184ET195Q/α3 mutant involved changes in

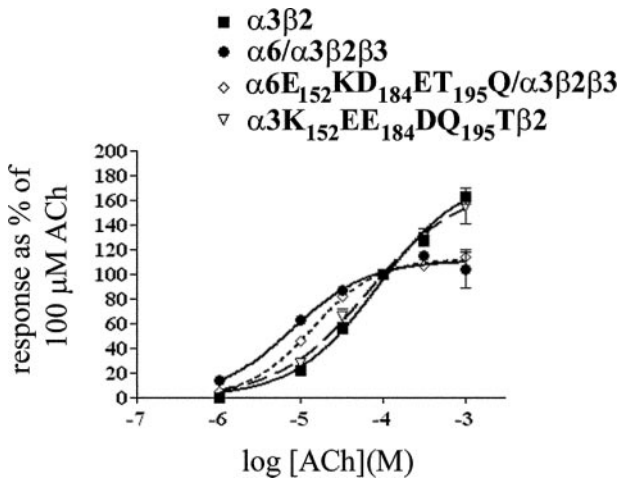

FIGURE 4. **ACh dose response on WT and mutant receptors.** Both mutant receptors exhibited similar sensitivity to acetylcholine relative to their WT counterparts. Values are mean ± S.E.M. from five to eight separate oocytes.

ACh affinity, ACh dose-response curves were obtained for the WT and mutant receptors. ACh activated the WT and mutant receptors with similar potencies, with an EC_{50} of 7.7 μM (95% CI: 5–12 μM) and 14 μM (95% CI: 12–16 μM) for the WT and mutant receptor, respectively (Fig. 4).

Next, the critical residues identified in the α6 subunit were substituted into α3 to assess for gain of function with respect to toxin susceptibility. Residues Glu-152, Asp-184, and Thr-195 of α6 were substituted for the homologous residues in the α3 subunit NTR. The resulting α3 mutant, designated as α3K152EE184DQ195T, was co-expressed with β2 subunit in oocytes. The α3K152EE184DQ195Tβ2 nAChR was ~150-fold more sensitive to α-CTX MII[S4A,E11A,L15A] compared with WT α3β2 nAChR (Table 4 and Fig. 3*B*), with no change in ACh sensitivity (EC_{50} on α3β2, 87 μM (CI: 62–121 μM); EC_{50} on α3K152EE184DQ195Tβ2, 64 μM (CI: 30–137 μM)) (Fig. 4).

α6 Residues Glu-152, Asp-184, and Thr-195 Interact with Other α6-Selective α-Conotoxins—We next investigated whether the identified residues were critical for the interaction with other α6*-selective conotoxins, specifically α-CTX PIA and α-CTX MII analogs α-CTX MII[H9A,L15A] and α-CTX MII[E11A]. When tested on α6E152KD184ET195Q/α3β2β3, all three peptides were less potent against the mutant than the WT α6/α3β2β3 nAChR (Table 5 and Fig. 5). Similarly, when tested on the mutant α3K152EE184DQ195Tβ2 nAChR, all three α-conotoxins were more potent in blocking the mutant than the WT α3β2 nAChR, although the gain in sensitivity was much less for α-CTX PIA than for the α-CTX MII analogs (Table 5 and Fig. 5).

Positive Charge at Position 152 Disfavors Interaction of the α3 Subunit with α-CTX MII[S4A,E11A,L15A]—Among the residues that affected the potency of α-CTX MII [S4A,E11A,L15A], there is a charge reversal, from Glu-152 in α6 to a Lys-152 in α3; the residue exchange caused an ~8-fold reduction in the potency of the peptide for the α6/α3 subunit. To determine whether this change in potency was due to a charge reversal or to a change in the side-chain length, α6Glu-152 was systematically replaced with an Arg, Gln, or Met. The Arg mutation retains the charge reversal, but has a longer side chain, whereas

TABLE 5

IC_{50} values for block by α-CTX PIA, α-CTX MII[H9A,L15A] and α-CTX MII[E11A] of WT and mutant nAChRs

Numbers in parentheses are 95% confidence intervals.

nACR	IC_{50} (95% CI)		
	α-CTX PIA	α-CTX MII[H9A,L15A]	α-CTX MII[E11A]
		nM	
α6/α3β2β3	0.95 (0.71–1.3)[a]	2.4 (1.7–3.4)[b]	0.16 (0.13–0.19)[b]
α3β2	74 (49–110)[a]	4900 (3500–6600)[b]	8.7 (6.8–11)[b]
α6/α3E152KD184ET195Qβ2β3	33 (28–40)	1500 (840–2700)	9.1 (6.9–12)
α3 K152EE184DQ195Tβ2	22 (19–25)	36 (30–43)	0.53 (0.40–0.71)

[a] Values for WT α6/α3β2β3 and α3β2 are from Ref. 18.
[b] Values for WT α6/α3β2β3 and α3β2 are from Ref. 19.

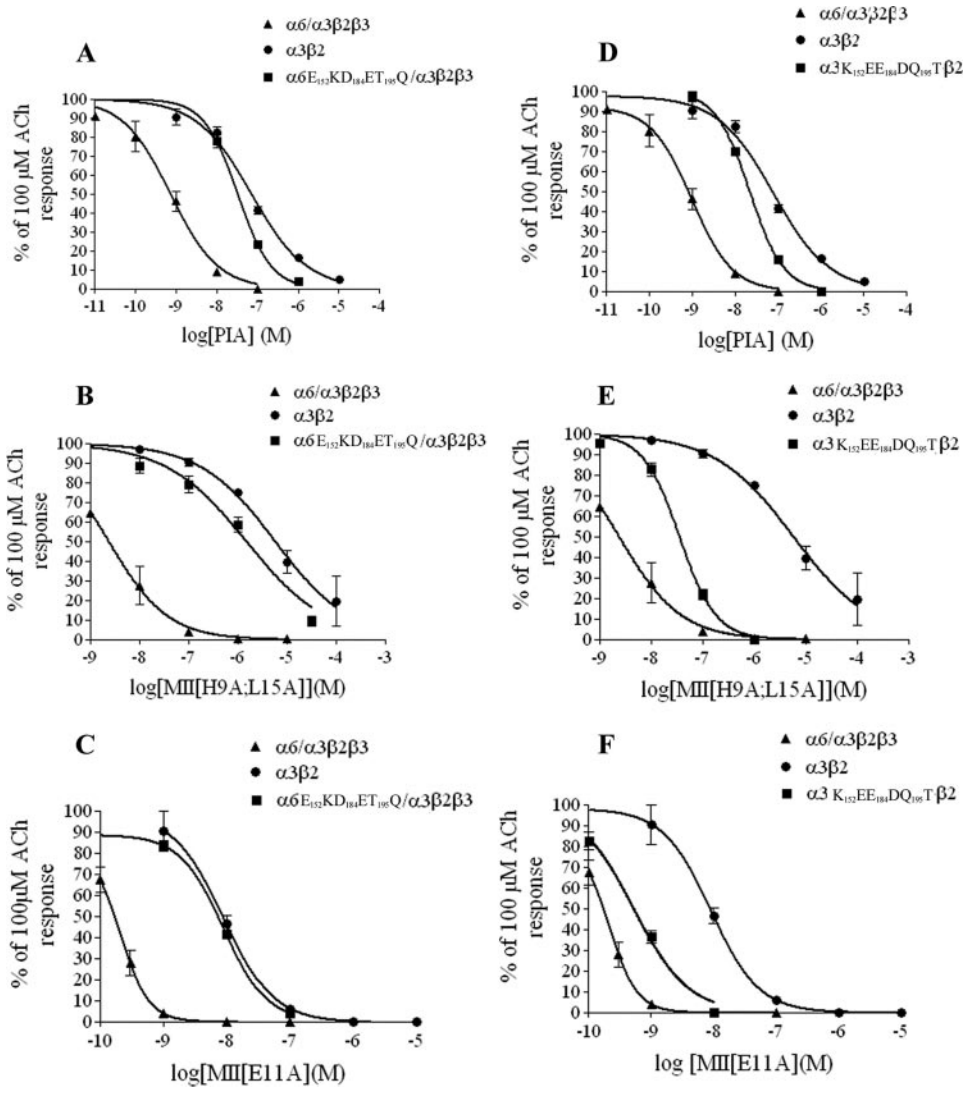

FIGURE 5. **Additional α6β2* selective analogs also markedly gain or lose activity with receptor residue substitutions.** *A–C*, change of α6 residues Glu-152, Asp-184, and Thr-195 to corresponding α3 residues caused a loss of sensitivity to inhibition by α-CTX PIA, α-CTX MII[H9A,L15A] and α-CTX MII[E11A]. *D–F*, the reciprocal replacement of α3 residues with the corresponding α6 residues led to an increase in sensitivity to block by the MII analogs, but to a lesser extent to α-CTX PIA block. Values are mean ± S.E.M. from three to five separate oocytes.

Gln replacement retains the side-chain length of Glu, but eliminates the negative charge. Met has a straight side chain, similar to Lys, but is not charged. As with the α6E152K/α3 mutant, the α6E152R/α3 mutant had a lower sensitivity to α-CTX MII[S4A,E11A,L15A] (IC_{50}: 23 nM (95% CI: 19–29 nM)) (Fig. 6). Both α6E152Q/α3 and α6E152M/α3 mutations only slightly changed the IC_{50} of the analog relative to the WT receptor, with IC_{50} values of 5.9 nM (95% CI: 5.0–7.0 nM) and 4.3 nM (95% CI: 3.5–5.5 nM), respectively (Fig. 6).

DISCUSSION

We have designed and synthesized a novel, high affinity ligand that discriminates between the closely related α6/α3β2β3 and α3β2 nAChRs. The new peptide is a triple mutation of α-CTX MII, with Ala substituted at positions 4, 11, and 15. The parent peptide, α-CTX MII, does not distinguish well between α3β2 and α6/α3β2β3 nAChRs. Conversely, the Ala-substituted peptide retained activity against α6/α3β2β3 nAChR, but dramatically lost activity against α3β2 nAChR, *i.e.* compared with α-CTX MII, the new peptide is only 3-fold less active against α6/α3β2β3 nAChRs but ~1700-fold less active against α3β2 nAChRs. These changes shift the selectivity ratio (IC_{50} α3β2:IC_{50} α6/α3β2β3) of 5.6 for the parent peptide to >1000 for the mutant, clearly indicating that the receptors can be well differentiated (Table 1).

Amino acid residues that determine the high potency of α-CTX MII for the α3 subunit were previously characterized and are Lys-185 and Ile-188 (17). However, both of these residues are conserved between the α3 and the α6 subunits, which helps explain the similar high affinity of α-CTX MII for α6/α3β2β3 and α3β2 nAChRs. In this study, receptor mutagenesis was used to assess the residues in the extracellular region of the α6 *versus* the α3 subunit that confer selectivity of the new peptide α-CTX MII[S4A,E11A,L15A] for the α6 subunit. These amino acids include Glu-152, Asp-184, and Thr-195. Receptors with α6 subunits in which all three residues

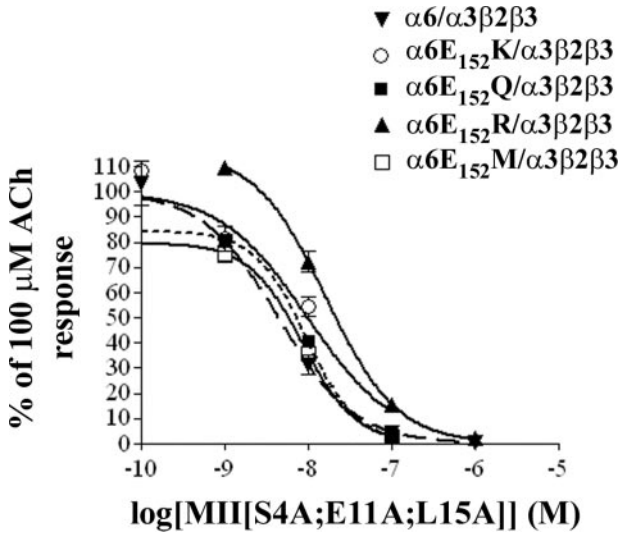

FIGURE 6. **Positive charge in position 152 adversely affects toxin binding.** Replacement of Glu-152 with Arg reduced activity of α-CTX MII[S4A,E11A,L15A] by 19-fold. In contrast, substitution of Glu-152 by Gln or Met did not have a large effect on potency. Values are mean ± S.E. from three to five oocytes.

were simultaneously exchanged with analogous residues of the α3 subunit had a >1000-fold higher IC_{50} for α-CTX MII[S4A,E11A,L15A]. Conversely, replacing residues in α3 with the three key α6 residues increased sensitivity for α-CTX MII[S4A,E11A,L15A] by ~150-fold.

Recent crystallographic structures of ACh binding proteins (AChBP) from *Lymnea stagnalis*, *Aplysia californica*, and *Bulinus truncatus*, which are used to model the nAChR in its ligand-bound state, as well as the high resolution structure of the *Torpedo* nAChR in the closed state, have aided greatly in understanding the ligand binding domain of nAChRs, and the structural changes that follow agonist and/or antagonist binding (20–23). The structures consist of an N-terminal α-helix, two-short 3_{10} helices, and a core of 10 β-sheets, β1–β10. An "aromatic cage" that forms the ACh binding pocket consists of loops A–F, with loops A–C belonging to the principal part (or the α subunit in case of muscle and neuronal nAChRs) and loops D–F belonging to the complementary part (the β subunit, in neuronal heteromeric nAChRs) (20, 23). It has been proposed that upon agonist (*e.g.* ACh) binding, loop C moves in a counterclockwise motion, closing on the agonist like a "hinge," thus capping and trapping the agonist (23–26). However, binding of an antagonist would lock the C-loop in an open (*i.e.* resting) conformation and prevent opening of the channel. The change in the C-loop conformation has been confirmed in high resolution crystal structures of α-CTX PnIA[A10L,D14K] and α-CTX ImI bound to AChBP from *A. californica* (21, 27).

Lys-185 and Ile-188, the two residues in the α3 subunit that interact with α-CTX MII (17), both reside in the β9 strand that precedes the C-loop, as determined from sequence comparison with both the *Lymnea* and *Aplysia* AChBPs (22, 27). Similarly, two of the residues that confer high selectivity of α-CTX MII[S4A,E11A,L15A] for the α6 subunit, Asp-184 and Thr-195, are in the β9 and β10 strands, respectively, the former precedes and the latter follows the C-loop (Fig. 7). Therefore, subtle differences in the geometry of the C-loop may affect toxin binding. α3Gln-195 has previously been shown to interact with α-CTX PnIA and κ-bungarotoxin, which block α3β2 nAChRs (28, 29). In addition, an Ile at this position in the *Aplysia* AChBP is involved in interaction with α-CTX ImI (27). The present study, however, indicates that α-CTX

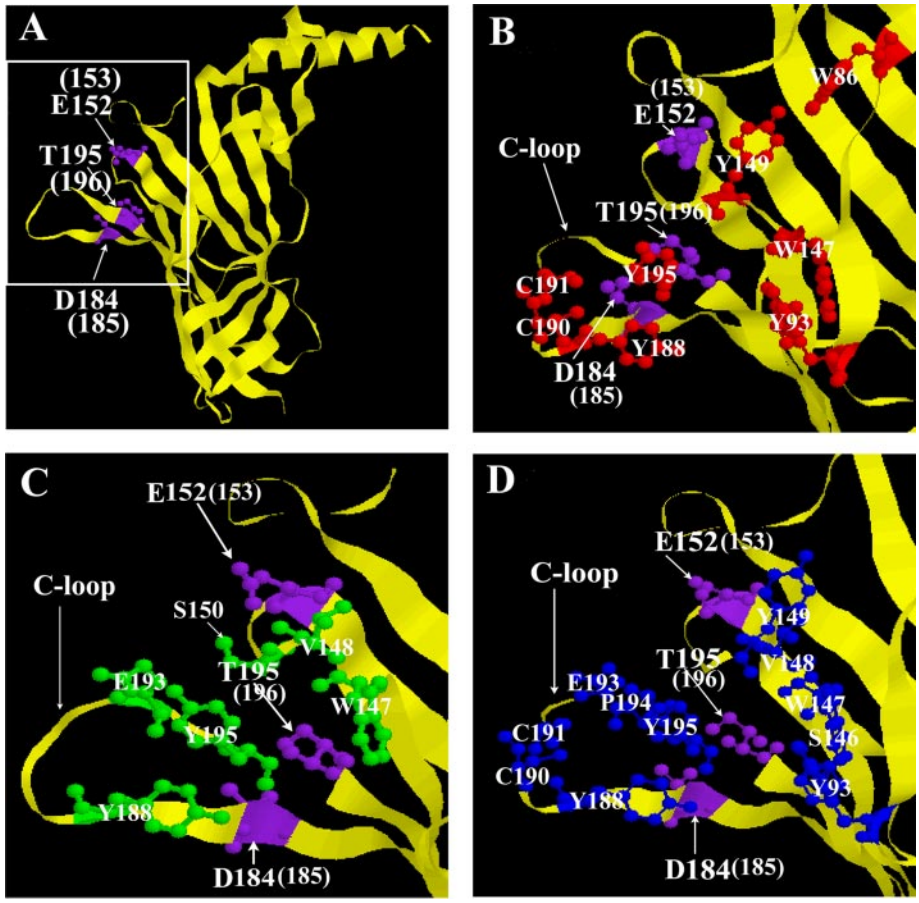

FIGURE 7. **Side view of a single subunit of the *Aplysia* AChBP (Protein Data Bank ID: 2BYP), with the C-loop shown in the "open" orientation as found when bound to an α-CTX.** *A*, the position of the homologous residues in the α6 subunit (*purple*) that interact with MII[S4A,E11A,L15A] were determined by alignment of the N-terminal extracellular region of α6 with a subunit of the *Aplysia* AChBP. The *numbers in parentheses* indicate numbering according to *Aplysia* AChBP. The *box* indicates the region that is enlarged in *B–D*. *B*, the residues that interact with acetylcholine (numbering according to *Aplysia* AChBP) are shown in *red* (the "aromatic cage"), and the residues of the α6 subunit that interact with α-CTX MII[S4A,E11A,L15A] are shown in *purple*. *C*, the residues of the *Aplysia* AChBP that interact with α-CTX PnIA(A10L and D14K) are shown in *green* (from ref. 21), and the residues of the α6 subunit that interact with α-CTX MII[S4A,E11A,L15A] are shown in *purple*. *D*, the residues of the *Aplysia* AChBP that interact with α-CTX ImI are shown in *blue* (from ref. 27), and the residues of the α6 subunit that interact with α-CTX MII[S4A,E11A,L15A] are shown in *purple*.

MII[S4A,E11A,L15A] prefers a Thr at this position, as found in the α6 ligand binding domain. Gln and Thr both have polar, but uncharged side chains. However, the side chain of Gln is longer than that of Thr. Therefore, it is possible that the slightly longer side chain of Gln-195 sterically hinders the binding of α-CTX MII[S4A,E11A,L15A] to the α3β2 nAChR. Similarly, Glu at position 184 of the α3 subunit may sterically hinder binding of the α-CTX MII analog, because the shorter Asp at this position, as found in the α6 subunit, favors the binding of the toxin.

The other residue in the α6 subunit that was found to influence the binding of α-CTX MII[S4A,E11A,L15A], Glu-152, although not directly in the β9–β10 sheets, lies in close proximity (Fig. 7). Additionally, this residue, which is in a homologous position to that of Glu-151 in the *A. californica* AChBP, has been shown to be critical for binding of the PnIA variant α-CTX PnIA[A10L,D14K] (21). Both the α3 and the α4 subunits, which are not sensitive to α-CTX MII[S4A,E11A,L15A], have a Lys at the homologous position. When the negatively charged α6Glu-152 is replaced with positively charged Lys or Arg, the resulting mutant is ~8 and 19-fold, respectively, less sensitive to α-CTX MII[S4A,E11A,L15A], suggesting that either the negative charge might be important for conferring high selectivity to the toxin, or that introduction of a positive charge might be unfavorable to binding of the toxin. To address the former possibility, α6Glu-152 was replaced with the isosteric, but uncharged Gln. This substitution caused an ~5-fold decrease in sensitivity to α-CTX MII[S4A,E11A,L15A], thus suggesting that the negative charge may have a role in conferring the high affinity of the toxin to the α6 subunit. To address the possibility that the introduction of a positive charge may be unfavorable, α6Glu-152 was replaced with Met, which is structurally similar to Lys but lacks the positive charge. This substitution caused a 3.5-fold decrease in the potency of the analog, as opposed to 8- and 19-fold decrease when either a Lys or Arg is present (see above), thus suggesting that the positive charge may contribute to the unfavorable interaction with the α-CTX MII[S4A,E11A,L15A].

In conclusion, we have created a high affinity MII analog that, unlike the parent peptide, is highly selective for α6/α3β2β3 over α3β2 nAChRs. Through receptor mutagenesis we have identified amino acid residues in the α6 subunit that are responsible for the differences in toxin affinity between these receptors. Considering the location of these residues with respect to residues that interact with ACh (Fig. 7*B*), it is likely that α-CTX MII[S4A,E11A,L15A] acts competitively to antagonize ACh binding. These residues are distinct from those previously determined as important to α-CTX MII interaction with the α3 subunit (17, 29) and provide further information for distinguishing among these structurally related nAChRs that have distinct roles in the peripheral and central nervous systems.

Acknowledgments—We thank Dr. Pradip Bandyopadhyay and Dr. Grzegorz Bulaj for helpful discussions.

REFERENCES

1. Lester, H. A., Dibas, M. I., Dahan, D. S., Leite, J. F., and Dougherty, D. A. (2004) *Trends Neurosci.* **27,** 329–336
2. Dani, J. A., and Bertrand, D. (2006) *Annu. Rev. Pharmacol. Toxicol.* **47,** 699–729
3. Le Novere, N., Zoli, M., and Changeux, J. P. (1996) *Eur. J. Neurosci.* **8,** 2428–2439
4. Azam, L., Winzer-Serhan, U. H., Chen, Y., and Leslie, F. M. (2002) *J. Comp. Neurol.* **444,** 260–274
5. Salminen, O., Murphy, K. L., McIntosh, J. M., Drago, J., Marks, M. J., Collins, A. C., and Grady, S. R. (2004) *Mol. Pharmacol.* **65,** 1526–1535
6. Azam, L., and McIntosh, J. M. (2005) *J. Pharmacol. Exp. Ther.* **312,** 231–237
7. Azam, L., and McIntosh, J. M. (2006) *Mol. Pharmacol.* **70,** 967–976
8. Perry, D. C., Mao, D., Gold, A. B., McIntosh, J. M., Pezzullo, J. C., and Kellar, K. J. (2007) *J. Pharmacol. Exp. Ther.* **322,** 306–315
9. Mugnaini, M., Garzotti, M., Sartori, I., Pilla, M., Repeto, P., Heidbreder, C. A., and Tessari, M. (2006) *Neuroscience* **137,** 565–572
10. Lai, A., Parameswaran, N., Khwaja, M., Whiteaker, P., Lindstrom, J. M., Fan, H., McIntosh, J. M., Grady, S. R., and Quik, M. (2005) *Mol. Pharmacol.* **67,** 1639–1647
11. Bordia, T., Grady, S. R., McIntosh, J. M., and Quik, M. (2007) *Mol. Pharmacol.* **72,** 52–61
12. Quik, M., Polonskaya, Y., Kulak, J. M., and McIntosh, J. M. (2001) *J. Neurosci.* **21,** 5494–5500
13. Quik, M., and McIntosh, J. M. (2006) *J. Pharmacol. Exp. Ther.* **316,** 481–489
14. De Biasi, M. (2002) *J. Neurobiol.* **53,** 568–579
15. De Biasi, M. (2002) *Curr. Drug Targets CNS Neurol. Disord.* **1,** 331–336
16. Cartier, G. E., Yoshikami, D., Gray, W. R., Luo, S., Olivera, B. M., and McIntosh, J. M. (1996) *J. Biol. Chem.* **271,** 7522–7528
17. Harvey, S. C., McIntosh, J. M., Cartier, G. E., Maddox, F. N., and Luetje, C. W. (1997) *Mol. Pharmacol.* **51,** 336–342
18. Dowell, C., Olivera, B. M., Garrett, J. E., Staheli, S. T., Watkins, M., Kuryatov, A., Yoshikami, D., Lindstrom, J. M., and McIntosh, J. M. (2003) *J. Neurosci.* **23,** 8445–8452
19. McIntosh, J. M., Azam, L., Staheli, S., Dowell, C., Lindstrom, J. M., Kuryatov, A., Garrett, J. E., Marks, M. J., and Whiteaker, P. (2004) *Mol. Pharmacol.* **65,** 944–952
20. Brejc, K., van Dijk, W. J., Klaassen, R. V., Schuurmans, M., van Der Oost, J., Smit, A. B., and Sixma, T. K. (2001) *Nature* **411,** 269–276
21. Celie, P. H., Kasheverov, I. E., Mordvintsev, D. Y., Hogg, R. C., van Nierop, P., van Elk, R., van Rossum-Fikkert, S. E., Zhmak, M. N., Bertrand, D., Tsetlin, V., Sixma, T. K., and Smit, A. B. (2005) *Nat. Struct. Mol. Biol.* **12,** 582–588
22. Hansen, S. B., Sulzenbacher, G., Huxford, T., Marchot, P., Taylor, P., and Bourne, Y. (2005) *EMBO J.* **24,** 3635–3646
23. Unwin, N. (2005) *J. Mol. Biol.* **346,** 967–989
24. Celie, P. H., van Rossum-Fikkert, S. E., van Dijk, W. J., Brejc, K., Smit, A. B., and Sixma, T. K. (2004) *Neuron* **41,** 907–914
25. Gao, F., Bren, N., Burghardt, T. P., Hansen, S., Henchman, R. H., Taylor, P., McCammon, J. A., and Sine, S. M. (2005) *J. Biol. Chem.* **280,** 8443–8451
26. Shi, J., Koeppe, J. R., Komives, E. A., and Taylor, P. (2006) *J. Biol. Chem.* **281,** 12170–12177
27. Ulens, C., Hogg, R. C., Celie, P. H., Bertrand, D., Tsetlin, V., Smit, A. B., and Sixma, T. K. (2006) *Proc. Natl. Acad. Sci. U. S. A.* **103,** 3615–3620
28. Luetje, C. W., Maddox, F. N., and Harvey, S. C. (1998) *Mol. Pharmacol.* **53,** 1112–1119
29. Everhart, D., Reiller, E., Mirzoian, A., McIntosh, J. M., Malhotra, A., and Luetje, C. W. (2003) *J. Pharmacol. Exp. Ther.* **306,** 664–670